# ANALYSIS OF THE ENERGETICS AND STABILITY OF LIQUID DROPLETS ON TEXTURED SURFACES WITH SQUARE MICROPILLARS

**Rahman M. A.* and Goswami A.**

*Author for correspondence
Department of Mechanical Engineering,
Bangladesh University of Engineering and Technology,
Dhaka 1000, Bangladesh
E-mail: ashiqurrahman@me.buet.ac.bd

## ABSTRACT

Numerous studies have established that roughening a hydrophobic surface can induce superhydrophobic properties on that surface. The suspended wetting state (Cassie-Baxter state) on a microtextured surface tends to collapse to a wetted state (Wenzel state) due to external stimulations. Multiple metastable Cassie-Baxter (CB) wetting states, separated by an energy barrier from Wenzel state, may also exist. In this study, 3D droplet models are developed to numerically investigate the shapes and energies of CB droplets residing on rough surfaces patterned with square pillars. A normalized form of droplet energy is used to compare the relative stabilities of metastable states. The sequence of stable droplet configurations with increasing droplet volume is analyzed for different isotropic wetting cases. Analysis reveals that wetting configuration with the most number of pillars at the drop-base suspends the biggest droplet with higher stability compared to other configurations. In order to explore droplet energetics on distinct substrates, the pillar width and spacing are varied in simulations. For the same drop-base area, the substrate that gives the least value of solid-fraction at the drop-base, characterized by its pillar width and spacing, suspends the biggest droplet as the most stable CB droplet compared to others.

## INTRODUCTION

In the realm of the physics of wetting, the surfaces are basically classified as hydrophilic and hydrophobic; depending on whether they attract or repel water drops. The contact angle made between the droplet's edge and the surface underneath it, gives a measure of these hydrophobic and hydrophilic properties. Smooth flat surfaces with appropriate surface chemistries are found to show maximum 'intrinsic hydrophobicity' of $120^o$ [1]. By incorporating micro-structures (e.g. micro-pillars, micro-grooves) on these hydrophobic surfaces, superhydrophobicity can be attained with a contact angle of greater than $150^o$ [2-3]. Superhydrophobic surfaces are of considerable interest for various technological applications due to its some noble properties, such as self-cleaning, anti-corrosion, and anti-icing etc.

## NOMENCLATURE

| | | |
|---|---|---|
| $A_{LS}$ | [$\mu m^2$] | Area of solid-liquid interface |
| $E$ | [μJ] | Free surface energy |
| $E_{norm}$ | [-] | Normalized form free surface energy |
| $f_S$ | [%] | Solid fraction at drop-base |
| $S_P$ | [μm] | Pillar Spacing |
| $V$ | [μL] | Volume of the droplet |
| $W_P$ | [μm] | Pillar width |

Special characters

| | | |
|---|---|---|
| $\theta$ | [$^o$] | Contact angle |
| $\gamma$ | [N/m] | Surface tension |

Subscripts

| | |
|---|---|
| *A* | Apparent |
| *CB* | Cassie-Baxter state |
| *i* | Intrinsic |
| *LA* | Liquid-air interface |
| *LS* | Liquid-solid interface |
| *SA* | Solid-air interface |

On micro-textured surface, droplets typically attain one of the two distinct wetting states: Wenzel wetting state [4] or Cassie-Baxter (CB) wetting state [5]. In Wenzel wetting state, the droplet enters into the asperities of the surface and a homogeneous contact exists between the droplet and substrate. In CB wetting state, the droplet does not enter into the asperities of rough surface rather it sits on a composite surface of air and solid. Generally, the equilibrium shape of a droplet represents its wetting configuration with the minimum energy state. However, in practice, drop does not always wet a surface following the absolute minimum energy state criteria. Depending on how the drop is formed, drop may attain a local minimum or a metastable state of the free surface energy [6]. Metastable composite state (advancing or receding) may be observed and pinning of the interface at the rim of the posts supporting the drop can prevent the transition to the Wenzel state unless the drop is externally perturbed [7]. These metastable composite states possess very high contact angles which is the basic requirement for a good superhydrophobic surface. Therefore, it is of technological importance to explore the relative stability of multiple metastable CB droplets on rough surfaces.

In recent years, enormous attention has been directed towards understanding the wetting phenomena and CB wetting states on micro-textured rough surfaces [8-18]. In an experimental study, Dubov *et al.* [11] investigated the effect of size of the droplet on the stability of CB wetting state through evaporation of the deposited droplets on rough silica surfaces. They found that on a given rough surface, a minimum size of droplet is required for the stability of composite wetting but their study was limited to circular pillar-patterned surfaces. Patankar *et al.* [12] experimentally explored the required pillar spacing to pillar width ratio for stable CB droplets on square pillar-patterned surface. Besides experimental studies, many theoretical models have been developed to analyze the stability of the CB state based on the principle of free energy [16-17]. In a recent study, Guo *et. al.*[17] developed a generic theory to calculate the critical pressure at which CB wetting state collapses on micro-textured surface. However, numerical methods are still less exploited to predict the relative stability of CB droplets on rough surfaces [14-15, 18]. Chen *et al.* [14] described a numerical method of calculating multiple metastable drop-shapes of anisotropic wetting on micro-grooved surfaces. Recently, Hao *et al.* [18] modeled CB droplet on square pillars and demonstrated that as the drop-size reduces, the contact line recedes on the top of pillars. However, their study was limited to droplet sitting on four pillars. Using a normalized form of droplet energy, Chatain *et al.* [15] numerically investigated the relative stability of multiple metastable CB drops on circular-pillar-patterned surfaces. There is still a lack of numerical schemes that can predict the stability of CB wetting state on microstructured surfaces and guide the design of superhydrophobic surfaces.

In the present study, the stability of CB droplets on square-pillar-patterned surfaces is investigated numerically using Surface Evolver (SE) [19]. The relative stabilities of the metastable droplets with different volumes under different wetting configurations are compared based on normalized form their interfacial surface energies. In addition, the effect of pillar width and spacing between pillars on the stability is explored extensively.

## MODEL FORMULATION AND METHODOLOGY

The model consists of a 3-D droplet placed on a square-pillar-patterned rough substrate. As the present study, is limited to micro-droplets (<10 μL), the gravitational effect is ignored. Then the total effective free surface energy of the sessile drop is given by

$$E = \iint_{A_{LS}} \gamma_{LS} dA + \iint_{A_{LA}} \gamma_{LA} dA + \iint_{A_{SA}} \gamma_{SA} dA \qquad (1)$$

where, $\gamma_{ij}$ is the interfacial tension between $i$ and $j$ phases, $A_{ij}$ is the interfacial area between $i$ and $j$ phases, and the subscripts, $L$, $A$, and $S$ stand for liquid, air and solid phase, respectively. For all the models, water was used as the liquid with a liquid-air interfacial tension ($\gamma_{LA}$) of 0.072 N/m at 25°C. The local intrinsic contact angle ($\theta_i$) of the substrate material for each homogenous area can be defined by Young's equation:

$$\gamma_{SA} - \gamma_{LS} = \gamma_{LA} \cos\theta_i \qquad (2)$$

Then, the droplet energy which needs to be minimized to achieve equilibrium shapes can be written as:

$$E = \gamma_{LA}[A_{LA} - \iint_{A_{LS}} \cos\theta_i dA] \qquad (3)$$

Hence, for a droplet with fixed volume and given liquid-air interfacial tension ($\gamma_{LA}$), the only material parameter needed to be specified is the intrinsic contact angle ($\theta_i$).

For numerical simulation, Surface Evolver, an interactive, finite-element-based public domain software, has been used. The software evolves a user-defined initial surface towards an ever-lower energy state. The required surface for simulation is generated by defining its vertices, edges and faces and then geometric, energy and volumetric constraints are applied to the vertices and edges of the surface. Detailed information concerning the theory and methods employed in this program is available in the SE manual [20]. In the present study, for CB droplets on substrate with square pillars, the free facets are given liquid-air interface energy, $\gamma_{LA}$. The difference between solid-liquid interfacial tension ($\gamma_{LA}$) and solid-air interfacial tension ($\gamma_{SA}$), which is equal to $-\gamma_{LA}\cos\theta_i$ according to Young's Law, is assigned to the pillar top facets (Figure 1). This energy assignment allows not to design the pillar height for the study of CB wetting state. The equilibrium shape of the numerical simulation is achieved by successive mesh refinements and energy minimizing iterative steps along with some intermediate vertex averaging techniques as shown in Figure 2. Repetitions of iteration were continued until the computed value of system's free energy stopped changing up to the first nine digits.

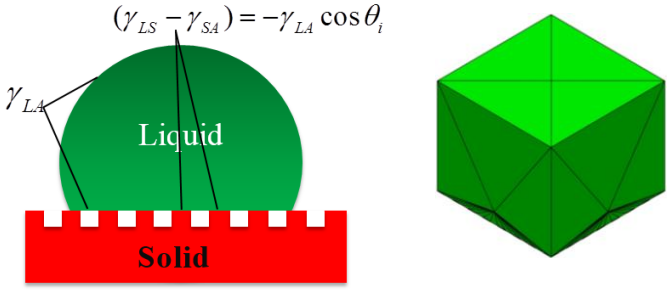


**Figure 1:** Model formulation: (a) schematic of surface energy assignment; (b) isometric view of initial cubical drop model.

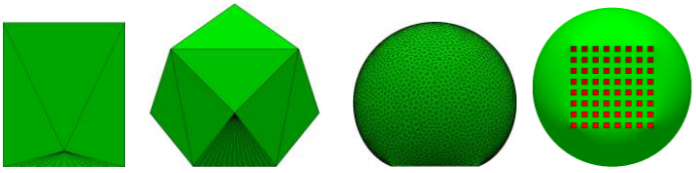


**Figure 2:** Drop attaining an equilibrium shape in Surface Evolver simulation: (a) front view of the initial model; (b) severel steps of iterations with initial mesh sizes; (c) equilibrium drop shape after successive mesh refinement and iterative steps; (d) rendered bottom view of the final equilibrium CB drop shape on square pillars.

## RESULTS AND DISCUSSION

The stability of CB droplets is studied by investigating the changes in the shape and energy of droplets as a function of droplet volume and the number of pillars at the drop-base. The interfacial surface energy that is minimized to get an equilibrium drop shape can be written in a normalized form as follows [15]:

$$E_{norm} = E \Big/ \gamma_{LA}(V^{2/3}) \qquad (4)$$

where, $V$ is the droplet volume. To explore the relative stabilities of multiple metastable CB drops on rough surface, their dimensionless energies i.e. $E_{\text{norm}}$ values can be compared as suggested by Chatain *et al.* [15]. On a smooth flat surface, the $E_{\text{norm}}$ value is found to be invariant for droplet of different volumes as shown in Figure 3(a). The apparent contact angle ($\theta_A$) of equilibrium drop-shape is equal to the intrinsic contact angle ($\theta_i$) for all droplets as displayed in Figure 3(b). If the surface chemistry i.e. the intrinsic contact angle ($\theta_i$) changes, the $E_{\text{norm}}$ value differs. Hence, on smooth flat surfaces, $E_{\text{norm}}$ is a function of the intrinsic contact angle ($\theta_i$) as shown in Figure 4.

Now, on the same flat surface, while the contact line of all droplets are kept fixed at contact line position of the equilibrium drop shape of 1µL, $E_{\text{norm}}$ becomes dependent on the droplet volume as shown in Figure 5(a). The normalized energy gets a minima for droplet size of 1µL and any other droplet results in a higher $E_{\text{norm}}$ value. Figure 5(b) displays that the droplets with a volume of less than 1µL manifest $\theta_A < 120^o$ and the droplets having volume greater than 1µL possess $\theta_A > 120^o$ due to their constrained contact line delimited by the contact line for the equilibrium position of droplet of 1 µL. Only the droplet of 1 µL attains stable equilibrium shape and all other droplets are metastable due to their constrained contact line. The non-equilibrium position of the contact line of the metastable droplets causes additional elastic energy to the droplet energy [15].

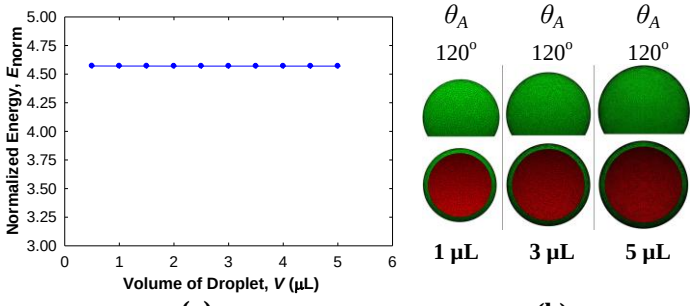


**Figure 3:** Droplets on smooth flat substrates: (a) Normalized Energy of a free sessile droplet with variation in droplet size for an intrinsic contact angle of 120°; (b) The front and bottom views of three simulated equilibrium. The red area constitutes the solid-air interface and its boundary line is the three phase contact line or triple line.

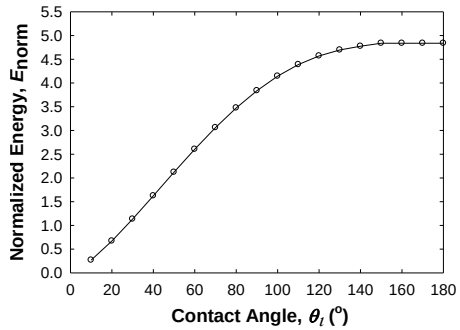


**Figure 4:** Normalized Energy of a free sessile drop as function of its intrinsic contact angle.

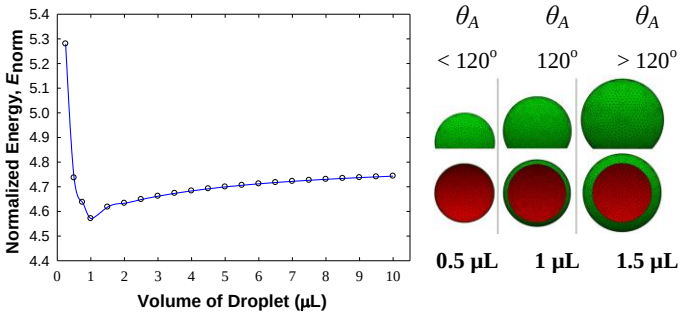


**Figure 5:** (a) Normalized energy of a sessile drop with an intrinsic contact angle of 120° as a function of drop volume, with the contact line fixed at the equilibrium position corresponding to a 1 µL droplet; (b) Front and bottom views of drops with volumes of about 1 µL.

The normalized energy of free and constrained sessile drops (from Figure 4 and 5(a), respectively) as a function of their apparent contact angles is compared in Figure 6. At the point of intersection, it is observed that the droplet which possesses the apparent contact angle equals to the intrinsic contact angle acts like a free sessile drop. Hence, when the $E_{\text{norm}}$ becomes function of droplet volume, the minimum $E_{\text{norm}}$ value represents the most stable droplet and all other $E_{\text{norm}}$ value corresponds to the metastable droplets. While the constraint of the contact line of the metastable droplets are released, the metastable drops with $\theta_A < 120^o$ or $\theta_A > 120^o$ will recede or advance, respectively, to attain the stable shape. Henceforth, the normalized energy concept is used to discuss the relative stabilities of the multiple metastable CB droplets on rough substrates with square micro-pillars.

Figure 7(a) shows a simulated CB droplet residing on square-pillar-patterned substrate confirming an isotropic wetting configuration. The intrinsic contact angle on the solid is 120°. A square wetting interface *ABCD* is formed at drop-base on total 64 pillars arranged in an '8x8' pillar arrangement i.e. in each direction of rectangular co-ordinates there is eight pillars. The constrained contact line passes through the boundary edges of the pillars confirming the complete wetting of the top surfaces of all pillars upon which the droplet remains suspended. For the validation and justification of the

assumption of the CB wetting state on the selected surface topography, the width and spacing of pillars are selected based on those found in the reported experimental studies in the literature for identical wetting condition [12]. The pillar width ($W_P$) is 20 μm and the pillar spacing ($S_P$) is 40 μm for the wetting configuration of Figure 5(a). This wetting configuration can be designated as $W_P^{20}S_P^{40}[8x8]$, and the droplet can be expressed as 'drop on 8x8 pillars'. Similar designations and expressions will be used throughout the remainder discussion.

Figure 7(b) displays the comparison of the normalized energies of liquid droplet residing on 8x8 pillars and that of a free sessile droplet on a smooth flat surface (similar to Figure 4) as a function of their apparent contact angles. The intersecting point of these two curves indicates that the most stable drop residing on 8x8 pillars has the same normalized energy as a free sessile drop on a smooth flat surface with an intrinsic contact angle of 158°. It means that an intrinsically hydrophobic surface ($\theta_A = \theta_i = 120^o$) turns into a superhydrophobic surface ($\theta_A > 150^o$) due to micro-textures. For the stable drop residing on 8x8 pillars, the area fraction ($f_s$) of solid at the drop base is found to be 13% from calculation of Surface Evolver. For CB wetting state of droplet, the equilibrium contact angle ($\theta_{CB}$) on micro-patterned solid substrate is given by

$$\cos\theta_{CB} = f_s \cos\theta_i - (1 - f_s) \qquad (5)$$

Using this equation, a solid fraction value of 13% along with an intrinsic contact angle of 120° gives the CB contact angle ($\theta_{CB}$) of 159° which is very close to the apparent contact angle of 158° obtained from the numerical study. This excellent agreement indicates that the stable drop on a micro-patterned surface possess an apparent contact angle that is equal to the equilibrium contact angle ($\theta_{CB}$) on that surface. Therefore, other metastable droplets on the surface has either be advancing or receding front with contact angles different from the equilibrium contact angle. It might also be noted in reference to the previous discussion of sessile drop on smooth flat surfaces that the most stable liquid droplet on this micro-textured substrate has an unconstrained contact line whereas all the other metastable droplets have constrained contact line.

Now, different configurations of droplets on micro-textured surface are explored for an extensive analysis. The substrate properties are taken based on those used in the experimental work of Patankar *et al.* [12] who demonstrated multiple metastable CB droplets on PDMS (Polydimethylsiloxane) substrate patterned with square pillars with an intrinsic contact angle of 114°. The water droplet sitting on the model surface with 20 μm pillar width and 40 μm pillar spacing for 8x8 pillar arrangement has been simulated for different isotropic composite wetting configurations. The surface chemistry and the properties of microstructures are fixed for all configurations whereas the number of pillars at drop base is systemically varied. Therefore, to confirm isotropic wetting case, square liquid drop base for all configurations has been designed and that institutes the configurations of pillar arrangements as 8x8 to 9x9, 10x10, 11x11, 12x12, and so on. A total of five configurations, $W_P^{20}S_P^{40}[8x8]$ to $W_P^{20}S_P^{40}[12x12]$ have been simulated for the present analysis.

Figure 8(a) displays the normalized energy curves as a function of the droplet volume for different simulated configurations. Each curve possesses a minima and has been constructed from the computed results ranged around its minimum energy value. As discussed earlier, minima in a normalized energy curve represents the most stable droplet size residing on that pillar arrangement. In case of stability, a given droplet of constant volume would reside more stably on the configuration which gives comparatively lower normalized energy. Figure 8(a) also displays that for a higher volume of liquid droplets, the normalized energy values for configurations with more pillars are lower than that of the configurations with fewer pillars. It means larger droplet requires more pillars on drop-base to be stable on. When the size of the drop increases it requires more contact area with the substrate i.e. greater drop-base with greater number of pillars for stable droplet. The bottom views of the stable droplet for different configurations are displayed in Figure 8(b) which reveals the relative size of the droplets. As we go from $W_P^{20}S_P^{40}[8x8]$ to $W_P^{20}S_P^{40}[12x12]$ for the specified PDMS substrate , the size of the stable droplet changes from 0.35 μL to 1.6 μL

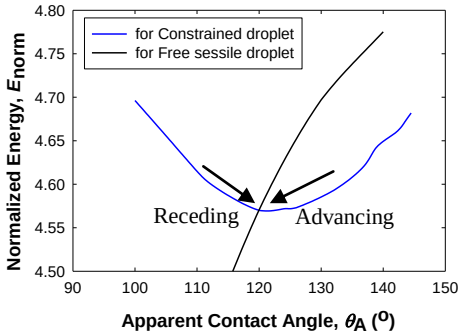


**Figure 6:** Comparison of the normalized energies of a constrained drop with $\theta_i = 120^o$ and that of a free sessile drop as a function of their apparent contact angles.

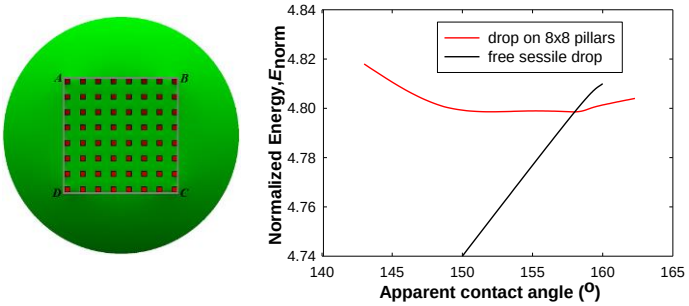


**(a)** **(b)**

**Figure 7:** (a) Rendered bottom view of a simulated CB droplet on a square array (8x8) of pillars and having a square wetting interface as indicated by ABCD; (b) Normalized energies of a droplet on micro-textured surface and that of a free sessile droplet as a function of apparent contact angle.

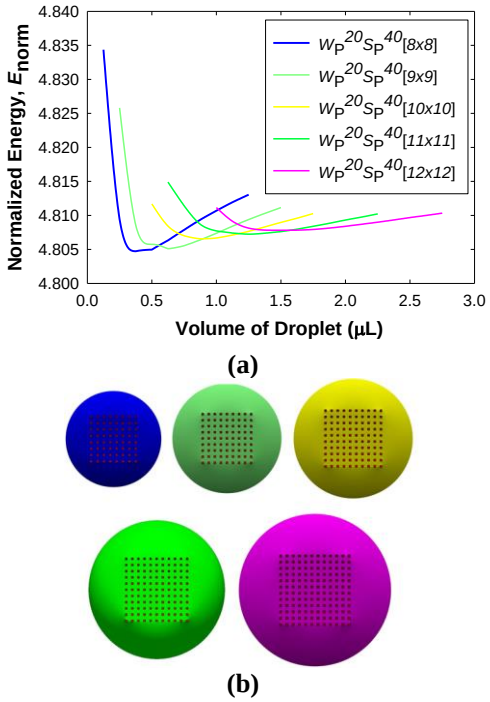


**Figure 8:** (a) Variation of normalized energy of droplets of different isotropic wetting configurations on a rough substrate patterned with sqaure pillars; (b) The bottom views of the different configurations; the color of the pictures of the droplet in (b) corresponds to the related energy curve displayed in (a).

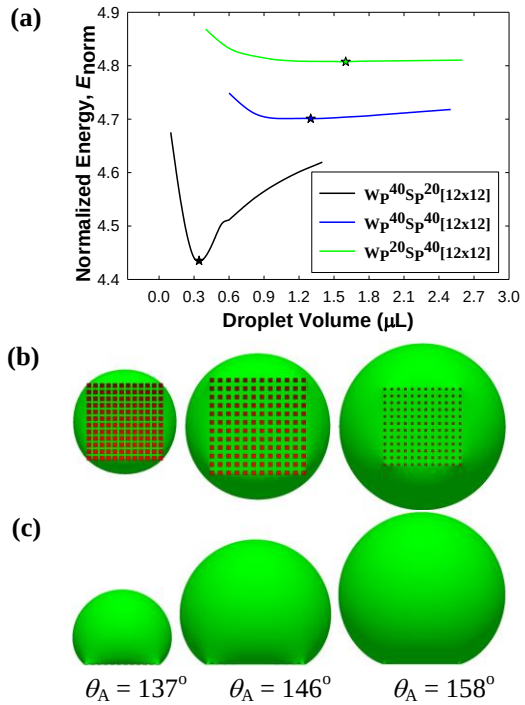


**Figure 9**: (a) Variation of normalized energy of droplets on the selected sample surfaces: $W_P^{40}S_P^{20}$[*12x12*], $W_P^{40}S_P^{40}$[*12x12*], and $W_P^{20}S_P^{40}$[*12x12*] ; (b) Bottom views of the most stable droplets; (c) Front view of the most stable droplets.

Droplet on pillar-patterned substrate possesses discrete contact lines. In the numerical simulation, pinning of the contact lines on the peripheral pillars occurred while the volume of the droplet was increased from the most stable size on one configuration. Due to the pinning of contact lines, the increase in droplet volume caused monotonic increase in the contact angles. Hence, the metastable advancing CB wetting mode with very high contact angle was observed. On the other hand, decrease in the droplet volume from the most stable size caused slip of contact lines on peripheral pillars i.e. receding CB mode became evident.

To investigate how the pillar width and spacing affects the stability of the CB droplets on the micro-textured surface, the analysis has been further extended to examine the size of the stable droplet on substrates with distinct pillar width and spacing. For this study, in order to cover a wide range of geometric space, three sample substrates were selected having a pillar width twice, equal, and half of the pillar spacing, respectively. The number of pillars at drop base are kept constant for all the three cases and the wetting configurations chosen for study are $W_P^{40}S_P^{20}$[*12x12*], $W_P^{40}S_P^{40}$[*12x12*], and $W_P^{20}S_P^{40}$[*12x12*], respectively. Figure 9(a) shows the variation of normalized energy as a function of drop volume for droplets on these three sample substrates. The points indicated by the 'star' symbols on the normalized energy curves represent the most stable droplet for the corresponding wetting configurations. Now, from the minima of the normalized energy curves for samples $W_P^{40}S_P^{20}$[*12x12*] and $W_P^{40}S_P^{40}$[*12x12*], it seems as the pillar spacing increases from 20 μm to 40 μm with all other parameters remaining constant, the size of the stable droplet residing on the sample surfaces increases from ~0.35 μL to ~1.3 μL. The drop-base area created by the constrained droplet on sample $W_P^{40}S_P^{40}$[*12x12*] is about two times greater than the drop-base area for sample $W_P^{40}S_P^{20}$[*12x12*] due to the increased pillar spacing as shown in Figure 9(b). Therefore, it can be assumed that the combination of pillar spacing and width which causes greater drop base area might suspend larger droplet as stable one compared to that for other combinations. However, for samples $W_P^{40}S_P^{20}$[*12x12*] and $W_P^{20}S_P^{40}$[*12x12*], though they manifest nearly the same drop-base area (Figure 9(b)), the volume of the stable drop on the latter being ~1.6 μL which is nearly four times of that (~0.49 μL) for the former sample surface. Calculation of the solid area fraction ($f_s$) at the drop-base shows that $f_s$ for sample $W_P^{40}S_P^{20}$[*12x12*] is about 47% which is about 13% for $W_P^{20}S_P^{40}$[*12x12*]. Hence, the solid fraction at drop base might play the vital role for the size of stable droplet on sample surface. Finally, comparison between samples $W_P^{40}S_P^{40}$[*12x12*] and $W_P^{20}S_P^{40}$[*12x12*] reveals that the latter gives higher droplet volume (~1.6 μL) for the stable wetting configuration in spite of having a smaller drop-base area compared to the former one (Figure 9(b)). The calculated $f_s$ at the drop-base for the two samples are found to be 27% for sample $W_P^{40}S_P^{40}$[*12x12*], whereas for sample $W_P^{20}S_P^{40}$[*12x12*], is 13%. Hence, from the comparisons it is evident that the area of the drop-base is not the main criterion for droplet stability; rather it is the variation of solid fraction due to topographical variation of the surface

which plays a more dominant role in determining the stability of the CB droplets. It might further be noted that according to the theory of Cassie-Baxter [5], the apparent contact angle of the stable droplet increases with a decrease in the value of the solid fraction ($f_s$). The findings of this numerical study, as shown in Figure 9(c), where the maximum apparent contact angle is found for the sample surface possessing the least solid-fraction, also exhibit a similar trend and hence are in good agreement with the theory.

## CONCLUSION

This study focused on investigating the dependence of stability of the suspended wetting state (Cassie-Baxter state) on the geometric variation of isotropic roughness features of solid substrates. It has been demonstrated that the energetics of wetting and the hysteresis of contact line provide a measure of the stability of the suspended droplets on these rough substrates. Due to the pinning and slip of the contact line on the pillars, multiple metastable Cassie-Baxter wetting states were obtained for a liquid droplet of constant volume. On a given micro-pillar-patterned surface, bigger droplet demands higher requirement of number of pillars beneath the droplet to get the most stable equilibrium Cassie-Baxter wetting state. For droplet on distinct substrates, the substrate that gives the lowest solid-fraction at the drop-base will suspend the largest droplet as the most stable suspended droplet. In general, the developed numerical simulations can significantly aid in engineering micro-patterns with the desired wetting behavior through optimizing the dimension, spacing and arrangement of the roughness features as well as to choose the appropriate surface chemistry.

## ACKNOWLEDGEMENT

The authors are grateful to Bangladesh University of Engineering and Technology (BUET) for providing the support to carry out this work.

## REFERENCES

[1] Cui X. S., Li W., On the possibility of superhydrophobic behavior for hydrophilic materials, *Journal of Colloid and Interface Science*, Vol. 347, 2010, pp. 156-162.

[2] Patankar N.A., Transition between superhydrophobic states on rough surfaces, *Langmuir*, Vol. 20, 2004, pp. 7097-7102.

[3] Chen Y., He B., Lee J., Patankar N. A., Anisotropy in the wetting of rough surfaces, *Journal of Colloid and Interface Science*, Vol. 281, 2005, pp. 458–464.

[4] Wenzel R. N., Resistance of solid surfaces to wetting by water. *Industrial and Engineering Chemistry*, Vol. 28, 1936, pp. 988–994.

[5] Cassie A. B. D., Baxter S., Wettability of porous surfaces. Transactions of the Faraday Society, Vol. 40, 1944, pp. 546–551.

[6] Barbieri L. , Wagner E. , and Hoffmann P., Water Wetting Transition parameters of Perfluorinated Substrates with Periodically Distributed Flat-Top Microscale Obstacles, *Langmuir*, Vol. 23 (4), 2007, pp. 1723–1734.

[7] Zheng Q. S., Yu Y., and Zhao Z. H., Effects of hydraulic pressure on the stability and transition of wetting modes of superhydrophobic surfaces. *Langmuir*, Vol. 21(26), 2005, pp.12207-12212.

[8] Callies M., Chen Y., Marty F., Pepin A., Quéré D., Microfabricated textured surfaces for super-hydrophobicity investigations, *Microelectric Engineering*, Vol. 78-79, 2005, pp. 100-105.

[9] Hans M., Müller F., Grandthyll S., Hüfner S., Mücklich F., Anisotropic wetting of copper alloys by one-step laser micro-patterning, *Applied Surface Science*, Vol. 263, 2012, pp. 416-422.

[10] Bhushan B., Jung Y. C., Micro and nanoscale characterization of hydrophobic and hydrophilic leaf surface, *Nanotechnology*, Vol. 17, 2006, pp. 2758–2772.

[11] Dubov A. L., Perez-Toralla K., Letailleur A., Barthel E., Teisseire J., Superhydrophobic silica surfaces: fabrication and stability, *Journal of Micromechanics and Microengineering*, Vol. 23, 2013, 125013 (8pp).

[12] He B., Patankar N.A., Lee J., Multiple equilibrium droplet shapes and design criterion for rough hydrophobic surfaces, *Langmuir*, Vol. 19, 2003, pp. 4999-5003.

[13] Promraksa A., Chen L. J., Modeling contact angle hysteresis of a liquid droplet sitting on a cosine wave-like patterned surface, *Journal of Colloids and Interface Sciences*, Vol. 384, 2012, pp. 172-181.

[14] Chen Y., He B., Lee J., Patankar N. A., Anisotropy in the wetting of rough surfaces, *Journal of Colloid and Interface Science*, Vol. 281, 2005, pp. 458–464.

[15] Chatain D., Lewis D., Baland J. P., Numerical analysis of the shapes and energies of droplets on micropatterned substrates. *Langmuir*, Vol. 22(9), 2006, pp. 4237–4243.

[16] Afferrante L., Carbone G., Microstructured superhydrorepellent surfaces: effect of drop pressure on fakir-state stability and apparent contact angles, *Journal of Physics: Condensed Matter*, Vol. 22(32), 2010, 325107 (13 pp).

[17] Guo H.Y., Li B., Feng X. Q., Stability of Cassie-Baxter wetting states on microstructured surfaces, *Physical Review E*, Vol. 94 (4), 2016, 042801 (15 pp).

[18] Hao J., Wang Z., Modeling Cassie-Baxter State on Superhydrophobic Surfaces, *Jounal of Dispertion Science and Technology*, Vol. 37(8), 2016, pp. 1208-1213.

[19] Brakke K. A., The surface evolver, *Experimental Mathematics*, Vol. 1(2), 1992, pp. 141–165.

[20] Brakke K. A., *Surface Evolver Documentaion*, 2013.

.